



ISSN: 0973-3469, Vol.18, No.(3) 2021, Pg. 305-317

## Material Science Research India

www.materialsciencejournal.org

# Anti-Inflammatory and Antioxidant Properties of *Coffea Arabica*/Reduced Graphene Oxide Nanocomposite prepared by green synthesis<sup>1213</sup>

D.S.M. PERERA<sup>1\*</sup>, R.C.L. DE SILVA<sup>1</sup>, L. D. C. NAYANAJITH<sup>1</sup>, H.C.D.P. COLOMBAGE<sup>1</sup>,  
T.S SURESH<sup>2</sup>, W. P. K. M. ABEYSEKERA<sup>3</sup> and I.R.M. KOTTEGODA<sup>1</sup>

<sup>1</sup>Materials Technology Section, Industrial Technology Institute,  
363 Baudhaloka Mw, Colombo 7. Sri Lanaka.

<sup>2</sup>Department of Biochemistry, Faculty of Medical Sciences, University of  
Sri Jayewardenepura, Nugegoda. Sri Lanka.

<sup>3</sup>Department of Biosystems Technology, Faculty of Technology, University of  
Sri Jayewardenepura, Homagama, Sri Lanka.

### Abstract

The present study focuses on an efficient eco-friendly method for reducing graphene oxide (rGO) using *Coffea arabica* leaf extract for bio-medical applications for the first time to the best of our knowledge. The reduction of graphene oxide (GO) using *Coffea arabica* leaves was verified through Raman, X-ray diffraction (XRD), Fourier transform infrared (FT-IR) spectroscopy, scanning electron microscopy (SEM). The XRD peaks corresponding to GO at  $2\theta = 10^\circ$  have disappeared on reduction of GO to rGO and the formation of rGO was verified through a new broad peak at  $2\theta = 26^\circ$ . FTIR revealed functional group changes in reducing GO to rGO. The SEM images of rGO showed a ribbed form instead of the rigid appearance of the GO flakes. The analysis revealed that the current green method is a feasible method for reducing GO to rGO and formation of the *Coffea arabica*/rGO nanocomposite. The composite prepared from young coffee leave exhibited higher antioxidant capacity than matured leave against scavenging 2,2'-azino-bis(3-ethylbenzothiazoline-6-sulfonic acid) (ABTS) and 2, 2-diphenyl-1-picrylhydrazyl (DPPH) free radicals. Fascinatingly, the *Coffea arabica*/rGO nano composite showed an anti-inflammatory activity as well suggesting that the *Coffea arabica*/rGO nano composite is promising candidate for bio-medical applications in near future.



### Article History

Received: 25 August  
2021

Accepted: 10 November  
2021


### Keywords

Ftir;  
Graphene Oxide;  
Green Synthesis;  
Nanocomposite;  
Reduced Graphene  
Oxide;  
Raman  
Sem;  
Xrd.

**CONTACT** D.S.M.Perera ✉ shashikaperera20@gmail.com 📍 Materials Technology Section, Industrial Technology Institute,  
363 Baudhaloka Mw, Colombo 7. Sri Lanaka.



© 2021 The Author(s). Published by Enviro Research Publishers.

This is an  Open Access article licensed under a Creative Commons license: Attribution 4.0 International (CC-BY).

Doi: <http://dx.doi.org/10.13005/msri/180306>

## Introduction

Coffee leaves have been used in food and medicine.<sup>1</sup> It has a long history in tropical medicinal application.<sup>2</sup> An attention has been gained for ethno-pharmacological applications due to its abundant bioactive phytochemicals such as phenolic acids, flavonoids, phytosterol, amino acids, alkaloids, carotenoids, terpenes, tannins, which are devoted to their anti-bacterial, anti-fungi, antioxidant, anti-hypertensive and anti-inflammatory activities. Type of plant species, growing region, climate, development stage, the age of the plant, collecting season and processing methods involved in coffee leaves affect phytochemical and bioactivities.<sup>3</sup>

Alternatively, graphene and reduced graphene oxide (rGO) has become one of the most remarkable scientific advances because of its outstanding properties and various applications including biomedical application. Graphene is a single layer of graphite while rGO is reduced form of GO. Various attempts have been used for preparing graphene including chemical vapor deposition, hydrothermal dehydration, epitaxial growth, mechanical routes, whereas chemical reduction of graphene oxide has been mainly followed to prepare rGO which is the easiest route for producing rGO.<sup>4</sup> However the chemical base methods utilize various hazardous chemicals including hydrazine, Sodium borohydrazine, dimethyl hydrazine, hydroquinones and ammonia.<sup>5</sup> Hydronic acid, which is highly corrosive, is used to obtain high quality rGO. Even trace amounts of final products pose harmful outcomes as they are highly toxic. As a result, the production of rGO, using natural reagents and eco-friendly methods have been captivated a huge attention in commercial applications.<sup>6</sup>

There is enormous number of green reductants, including amino acids, glucose, vitamin C, various plant extracts including caffeine, bacteria and organic acids are potential to reduce GO.<sup>6,7</sup> Although there are several studies on reduction of GO by coffee beans, there is no work reported on reduction with coffee leaves which is not seasonal like coffee beans. Therefore, studying on the reduction of GO using coffee leaves thought to be an important area needs investigation. Besides, the advantage of using both coffee leaves and rGO in biomedical application is achievable.

Roasting coffee beans during coffee bean production result in loss of considerable amount of chlorogenic acids in coffee beans. Mangiferin and chlorogenic acid with numerous health benefits found only in *Coffea arabica* leaves and not in coffee beans.<sup>1</sup> Coffee leaves are also considered to be a better antioxidant source than tea. Hence, they are more suitable for manufacturing novel natural pharmaceutical products.<sup>3</sup>

Considering the benefits of coffee leaves and rGO in biomedical applications and advantages of eco-friendly preparation methods, the present study focus on investigation of anti-oxidant and anti-inflammatory properties of coffee leave-rGO nanocomposite prepared through green synthesis approach.

## Experimental

### Plant Materials and Chemicals

*Coffea arabica* young leaves (one to three weeks old) and mature leaves (four to six months old), which were named as YC and MC respectively, were collected from the western province of Sri Lanka during the period of April to May, 2019. The plant was identified and authenticated by the curator of the National Herbarium, Royal Botanical Garden, Sri Lanka. Natural graphite (NG) (99.9% purity) was obtained from the Kahatagaha graphite mine in Sri Lanka. All other chemicals were provided by Sigma –Aldrich.

### Preparation of Reduced Graphene Oxide

The improved Hummers method was used to prepare graphite oxide (GO).<sup>8-11</sup>

The *Coffea arabica* (*C. arabica*) extract was prepared using clean, finely grinded young and matured leaves which were mixed with distilled water, boiled and filtered to obtain the *C. arabica* extract.<sup>7</sup>

The rGO was prepared as follows. The coffee leaves extract (Orange colour in Figure 4-1) was added into GO solution (1mg/ml) in a ratio of 1:1 (v/v) in 500 ml flask. The young leaf extract was sonicated at 40°C for 2 hrs and the mature leaves were sonicated at 60°C for 4.5 hrs. The colour of the mixture started to change from brown to black due to the reduction of graphene oxide. Ultimately, a homogeneously dispersed black colour solution of rGO formed

was washed several times with distilled water to remove the remaining plant extract and unbound molecules after reduction. For chemical reduction, 25% ammonia solution was added to the GO solution (1mg/ml) until the pH of the solution rose to pH12 and the mixture was sonicated at 80°C for 6hrs.<sup>12</sup>

### Characterization

The structure, morphological shape, and functional groups of the synthesized GO, rGO, and *C.arabica*/rGO composite were analyzed using XRD, SEM, FTIR and Raman spectroscopy. X-ray Diffractometer (Rigaku-ultima IV) with Cu K $\alpha$  ( $\lambda$  = 1542 Å) radiation, was used to analyze the structure of the composite. The functional groups were determined using Fourier Transformed Infrared Spectroscopy (FT-IR) (Bruker Tensor 27). A Scanning Electron Microscope (SEM) (Leo 1420vp) was used to determine the morphology. Raman (DXR2 SmartRaman thermo Scientific) spectrometer was used to analyze structural changes of GO.

### DPPH Radical Scavenging Activity

First, GO and *C.arabica*/rGO composite samples (5.00 mg) were vortexed to extract them into methanol (1.00ml) and centrifuged to remove insoluble particles.

The DPPH radical scavenging assay was performed according to the method described by Blois, (1958) in 96 well micro-plates.<sup>13</sup> Reaction volumes of 200  $\mu$ l, containing 125  $\mu$ M of DPPH radical and 50  $\mu$ l of different concentrations of GO and *C.arabica*/rGO composites, were incubated at 25  $\pm$  2°C for 15 minutes. The absorbance was recorded at 517 nm. Five different concentrations of 50  $\mu$ l of Trolox were used to construct the standard curve. The results were expressed as mg of Trolox per 1 g of extract and 1 g of dry weight of GO, YC/rGO or MC/rGO.

### ABTS Radical Scavenging Activity

First, GO and *C.arabica*/graphene composite samples (5.00 mg) were vortexed to extract into potassium persulfate (1.00ml) and centrifuged to separate the solid.

The ABTS<sup>•+</sup> radical scavenging assay was performed according to the method described by Re *et al.* (1999) in 96 well micro-plates.<sup>14</sup> A stable stock solution of ABTS radical cation was produced by reacting 10

mM of ABTS with potassium persulfate at 37°C for 16 hrs in the dark. The reaction volume of 200  $\mu$ l containing 40 $\mu$ M of ABTS<sup>•+</sup> radical and 50 $\mu$ l of different concentrations of GO and *C.arabica*/graphene composite extracts were incubated at 25  $\pm$  2°C for 10 minutes. The absorbance was recorded at 734 nm. Five different concentrations of 50  $\mu$ l of Trolox were used to construct the standard curve. The results were expressed as mg of Trolox per 1 g of extract and 1 g of dry weight GO, YC/rGO or MC/rGO.

### Membrane Stabilizing Activity

Rabbit blood (10ml) was purchased from the Medical Research Institute, Sri Lanka.

The anti-inflammatory assay is performed using the human red blood cell membrane stabilization method described by G. Leelaprakash, SM Dass, 2011<sup>15</sup> and Perez (1995) (16) with minor modifications.

The blood is collected from a healthy rabbit and transferred to the centrifuge tubes. The tubes are centrifuged at 3000 rpm for 10min and are washed three times with equal volume of normal saline. The washed red blood cells (RBCs) are reconstituted as a 10% v/v suspension with normal saline. The reaction mixture (2ml) consists of a 1 ml test sample of different concentrations (1200-200 $\mu$ g/ml) and 1 ml of 10% RBCs suspension. Instead of a test sample, only saline is added to the control test tube. Aspirin is used as a standard drug. All the centrifuge tubes containing the reaction mixture are incubated in a water bath at 56°C for 60min. At the end of the incubation, the tubes are cooled under running tap water. The reaction mixture is centrifuged at 3000 rpm for 5min. The absorbance of the supernatants is taken at 560 nm. The experiment was performed in triplicate for all the test samples. The percentage of membrane stability is calculated as follows:

Percentage membrane stability = (Abs control – Abs sample) X 100/ Abs control

### Results and Discussion

Green techniques have been recommended in this study due to their environmental friendliness and low cost. Moreover, it is exciting to be aware that the reaction's progress from GO to its reduced form

can be determined based on the changes in the color of the solution. Initially, the reaction mixture is brownish-yellow in colour [Figure 1 (b)]. And finally, it turns to a darkish black [Figure 1 (d)].

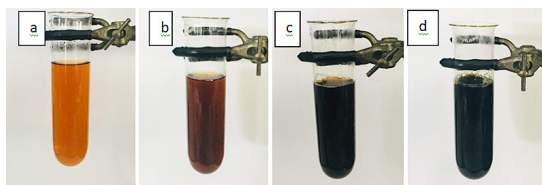


**Fig.1: (a) YCL extract (b) GO+YCL mixture, (c) After 1hrs at 40°C for GO+YCL mixture (d) After 2hrs at 40°C for GO+YCL mixture**

The GO reduction was carried out at different temperatures as well as under sonicated conditions. Comparing young and mature *C.arabica* extracts in GO reduction, the young leaf extract was faster than

the mature leaf extract, which is obviously due to higher polyphenol content in younger coffee leaves than mature leaves(3). Reduction temperature and time consumption were given in Table 1. With a young *C.arabica* extract, it was also discovered that GO required lower reduction temperatures because the activation energy required for GO reduction is higher at low temperatures. At the end of the reduction, the colour of GO and phytoextracts changed from brown to black. And homogeneous dispersion of reduced GO was observed without any aggregation. In the case of reduction, 5g of fine powder of *C.arabica* leaves was found to be adequate to reduce the given GO. Furthermore, it was discovered that increasing the amount of *C.arabica* had no effect on the reduction time. And the *C.arabica* extract acted as the only reductant in the solution.

**Table 1: Time taken by phytoextracts for reduction of GO**

Phytoextract	Sonicated Temperature/°C	Duration Required/hrs
1. Young <i>C.arabica</i> leaf extract	40	2
2. Mature <i>C.arabica</i> leaf extract	60	4.5

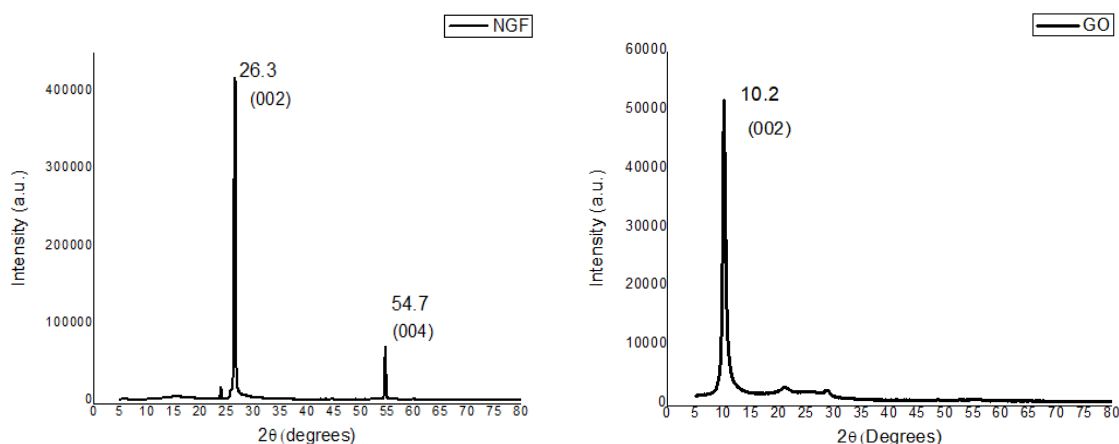


**Fig. 2: XRD spectra patterns of graphite and GO**

The adsorption of oxidized coffee polyphenols onto graphene suggested a result of steric hindrance within the graphene sheets, keeping them stably dispersed in water. Because of the complex structure of coffee polyphenols, the oxidation mechanism of coffee polyphenols is very complicated and depends on the oxidizer type and oxidization conditions, which need a great deal of study.

The Synthesis of GO from natural graphite flakes (NGF) was confirmed by X-ray diffraction analysis and removal of oxygen containing functional groups of GO has been showed by using Raman and FTIR analysis as shown later.

XRD patterns of natural graphite and GO are shown in Figure 2 (a,b).The characteristic peak (002) at

$2\theta=26.3^\circ$  corresponding to an interlayer distance of 0.34 nm of graphite. Moreover, it shows another peak at a  $2^\circ$  value of  $54.7^\circ$  for graphite (004).<sup>17</sup> Figure 3b shows the appearance of new sharp peak at  $2^\circ = 10.2^\circ$  corresponding to GO, which is the (002) plane with an interlayer distance of 0.76 nm. Due to the formation of oxygen function groups on the bulk graphite surfaces, the interlayer distance of GO has increased from 0.34 to 0.76nm.<sup>18</sup>

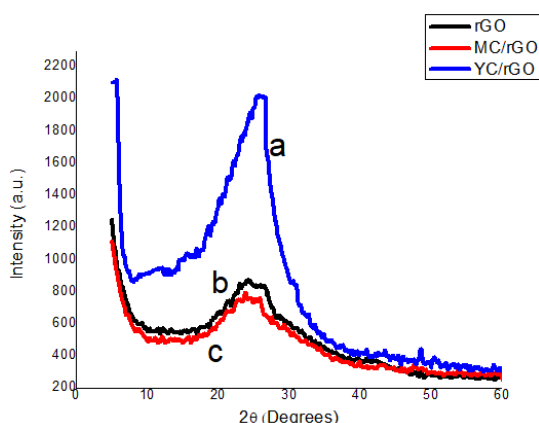


**Fig. 3: XRD patterns of (a) YC/rGO, (b) rGO and (c) MC/rGO**

XRD spectra of chemically reduced rGO, young *C.arabica*-reduced graphene composite (YC/rGO) and matured *C.arabica*-reduced graphene composite (MC/rGO) are shown in Figure 3.

To get a better understanding, the XRD pattern of reduced GO has been compared with the ammonia (chemically) reduced GO (rGO) as shown in Figure 3 (a,b,c). From the spectra of rGO and all phytoextracts reduced GO, it became cleared that the used *C.arabica* extracts have comparable potential to reduce GO as ammonia.<sup>5</sup> The GO was subjected to reduction using synthesized *C.arabica* leaf extracts. The shifting of diffraction peaks from  $\sim 10^\circ$  to  $\sim 26^\circ$  confirmed the reduction of GO. There were two different extracts due to the age of the *C.arabica* leaves. Polyphenol content may vary due to the age of the leaves. The results certainly reveal the formation of exceptionally organized few layer graphene (rGO) with an interlayer spacing of 0.33 nm<sup>18</sup> which is the characteristic peak of rGO. It reveals both *C.arabica* extracts have the potential to reduce GO, which leads to the formation of few-layer rGO sheets.

When comparing the two peaks of YC/rGO and MC/rGO, MC/rGO has a close relationship with chemically reduced rGO. The highest intensity rGO peak was exhibited by YC/rGO composite  $\sim 10$  showed efficient removal of oxygen containing group of GO.<sup>20</sup>

Generally, coffee polyphenols have been used as a highly efficient and environmentally friendly stabilizer and reducer for GO. The results from XRD of rGO in Figure 3 clearly reveal an efficient reduction of GO by coffee polyphenols.

The FTIR spectrum of graphite indicates no characteristic peak for the functional groups, due to the absence of oxygen functional groups.<sup>20</sup> After oxidation of graphite to GO, the GO reveals exceptional characteristic peaks, as shown in Figure 4(a). These consist of a wide band of O-H stretching vibration from the hydroxyl group, between 3000-4000  $\text{cm}^{-1}$ . The C=O stretching peak appeared at 1720  $\text{cm}^{-1}$ , C-O-C stretching peak appeared at 1204  $\text{cm}^{-1}$  was corresponding to the C-O stretching.<sup>21</sup> When comparing the obtained graphs of GO (a), YC/rGO (b) and MC/rGO (c) in figure 5, it showed a successful reduction of GO by *C.arabica* leaf extract without a stabilizer. All the prominent peaks of GO became weaker. The peaks (1720  $\text{cm}^{-1}$ ) attributed to C=O stretching have disappeared. The sharpness of the wide band for the hydroxyl group stretching between 3000-4000  $\text{cm}^{-1}$  has been decreased. A new C=C stretching peak appeared at 1614  $\text{cm}^{-1}$  corresponding to graphite. The peak of the O-H deformation and the water interlayer bending vibration are located at 1359  $\text{cm}^{-1}$ .<sup>22</sup>

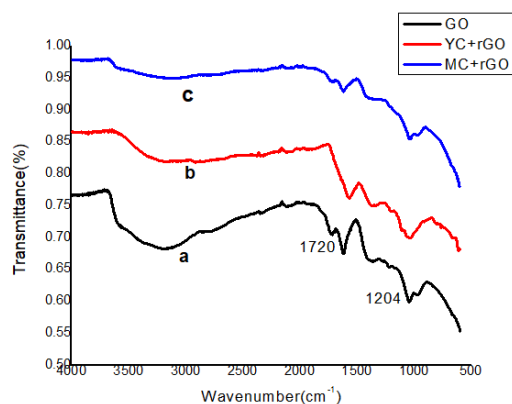


**Fig. 4: FT-IR spectra of (a) GO, (b) YC/rGO and (c) MC/rGO**

FTIR spectrum of YC/rGO in Figure 4b shows peaks 2850-3000  $\text{cm}^{-1}$  were due to the C-H stretching vibration. The peak at 1600-1670  $\text{cm}^{-1}$  was attributed to C=C stretching, confirming the reduction of and forming rGO successfully in the YC/rGO composite. The peak at 1376  $\text{cm}^{-1}$  was attributed to the O-H

bending of phenol groups.<sup>23</sup> Here, GO was called reduced GO due to the presence of peaks at 1025 and 1200  $\text{cm}^{-1}$ , which were related to the C-O stretching and due to the still remaining oxygen functional groups. This implies elimination of most of the oxygen containing groups from rGO.<sup>24</sup>

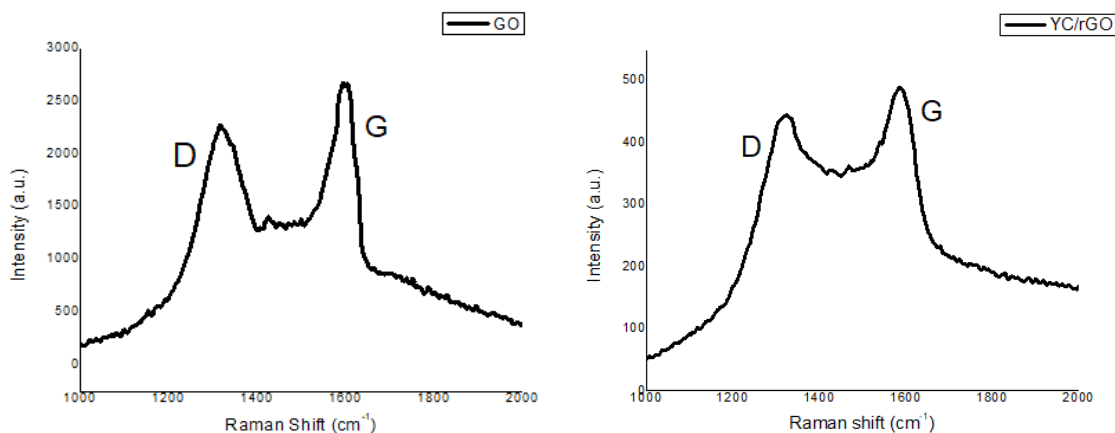


Fig. 5: The Raman Spectra of GO and YC/rGO

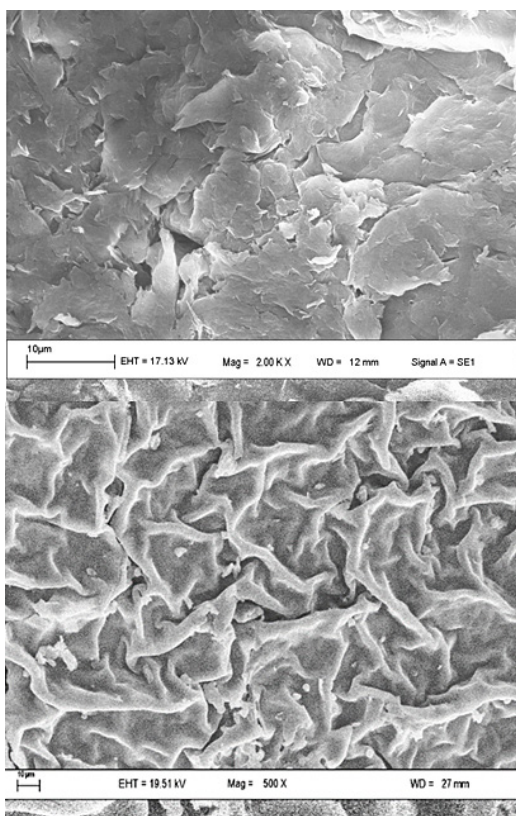


Fig. 6: The SEM images of GO and YC/rGO

Figure 5 shows Raman analysis of GO and *C.arabica*-reduced GO (YC/rGO) used to confirm the structural changes in the green reduced GO. The Raman spectra of rGO shows D peaks at  $\approx 1350 \text{ cm}^{-1}$  and G peaks at  $\approx 1590 \text{ cm}^{-1}$  ensuring the lattice distortions. The ID/IG peak intensity ratios are about 0.8 and 0.9 for GO and YC/rGO, respectively, confirming the reduction in the average size of  $\text{sp}^2$  domains and edge defects as a result of some C=C bond reduction in graphene oxide.<sup>25</sup> Moreover, it was found that a higher ID/IG ratio indicates fewer oxygen groups.<sup>11</sup>

The SEM images of GO and YC/rGO in Figure 6 depicts the rigid appearance of GO flakes as well as the corrugated silky cloth-like appearance of YC/rGO as a result of the formation of thin rGO layers. After splitting into thin layers, this wavy form is common in thin materials.<sup>26</sup>

In the laboratory, antioxidant activity can be assessed with the aid of measuring the direct reaction changes of antioxidant molecules with sufficiently stable free radical models. In this study, ABTS<sup>•+</sup> and DPPH were used as free radical models. Table 2 shows results for standard radicals ABTS<sup>•+</sup> and DPPH<sup>•</sup>.

When considering the ABTS radical scavenging assay, ABTS<sup>•+</sup> was generated through a reaction between potassium persulfate and ABTS. The reaction leads to produce blue/green ABTS<sup>•+</sup> chromophore with strong absorbance at wave length

of 734nm. A stable form of radical was generated prior to the response with antioxidant molecules. Decolouration was observed as in figure 7, after reaction with antioxidant molecules present in the reaction mixture.<sup>27</sup>



**Fig. 7: Micro plate after the ABTS radical scavenging assay of rGO**

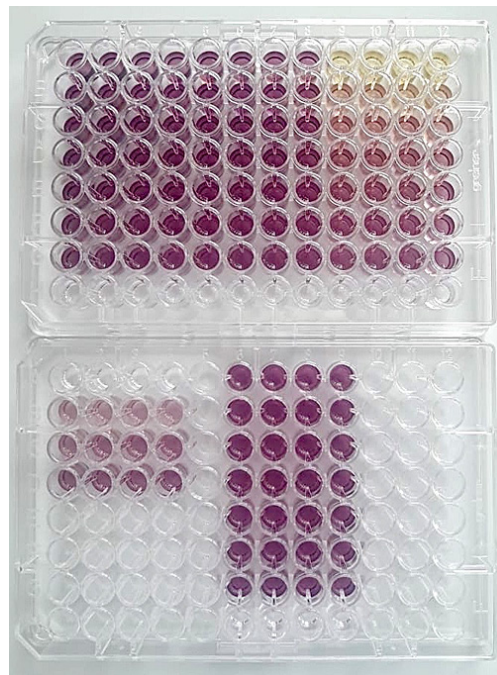


**Fig. 8: Micro plate after DPPH radical scavenging assay of rGO**

In this study, the organic nitrogen radical, DPPH, was used. It was purple in colour and showed maximum absorbance at a wavelength of 517 nm. A yellow

colour was observed after reaction with antioxidant molecules present in the reaction mixture, as in figure 8.

**Table 2: Antioxidant activity of YC/rGO and MC/rGO and GO**

Sample	Antioxidant activity			
	ABTS (IC50 $\mu\text{g/ml}$ )	DPPH (IC50 $\mu\text{g/ml}$ )	ABTS( $\mu\text{g Trolox equivalents/g of sample}$ )	DPPH( $\mu\text{g Trolox equivalents/g of sample}$ )
YC/rGO	155.28 $\pm$ 2.16	598.81 $\pm$ 7.70	326.21 $\pm$ 6.06	81.65 $\pm$ 12.62
MC/rGO	277.31 $\pm$ 3.08	3578.05 $\pm$ 9.64	183.85 $\pm$ 3.00	16.22 $\pm$ 4.66
GO	1344.38 $\pm$ 6.12	8945.07 $\pm$ 6.16	38.01 $\pm$ 2.17	5.55 $\pm$ 0.55

The results of ABTS and DPPH antioxidant properties of GO, YC/rGO and MC/rGO are shown in Table 2. Among all the determined antioxidant properties of GO, YC/rGO and MC/rGO have shown

significant differences ( $p < 0.05$ ). When comparing the two assays, all the samples have proven an appreciably higher ABTS radical scavenging activity than the DPPH radical scavenging activity. Those

molecules that are interested in ABTS scavenging may not be interested in DPPH scavenging. Alternatively, it could be due to a variety of factors, such as the solubility of sample molecules in various testing systems and the stereo selectivity of the radicals. And it was observed that YC/rGO and MC/rGO were more soluble in testing systems than GO. Chemically reduced GO was not soluble in testing systems, since its antioxidant activity is negligible in both assays. Actually, the antioxidant activity of reduced GO has no longer been properly studied.<sup>6</sup> Another reason for the difference in ABTS and DPPH scavenging ability is due to the stoichiometry of ABTS and DPPH with antioxidant molecules in the testing system.

Data represented as mean  $\pm$  SEM. ABTS and DPPH (n=4); Data in same column not sharing same letters significantly differ (P < 0.05). YC/rGO: young *C.arabica* reduced graphene oxide composite, MC/

rGO: matured *C.arabica* reduced graphene oxide composite, GO: graphene oxide.

When comparing the antioxidant activity of the two Nanocomposites, YC/rGO shows higher activity than MC/rGO, as shown in Figure 9. The difference between those two composites is the age of the *C.arabica* leaves used to reduce GO. It has been shown that the age of *C.arabica* leaves has a higher impact on antioxidant activity<sup>3</sup> as a result of the phytochemicals present in the leaves, particularly phenols such as caffeic, chlorogenic, iso-mangiferin, quercetin, mangiferin, rutin, catechin and epicatechin etc.<sup>28</sup> The phenolic content of young coffee leaves is higher than that of mature coffee leaves. Accordingly, the antioxidant activity is higher in young coffee leaves than of matured one.<sup>29,30</sup> That correlation can also be found in these YC/rGO and MC/rGO nanocomposites.

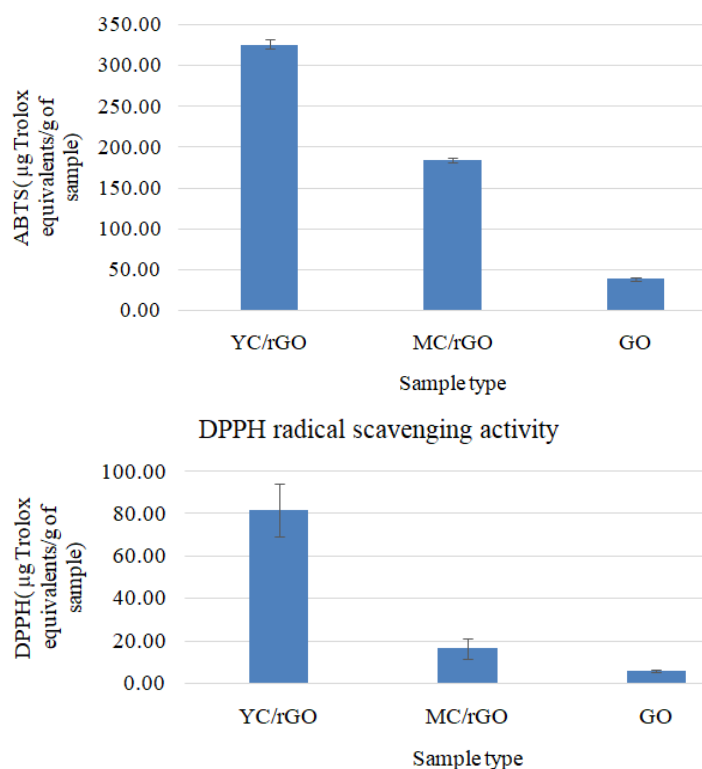


**Fig. 9: ABTS Trolox equivalent antioxidant capacity and DPPH Trolox equivalent antioxidant capacity. Data represented as mean  $\pm$  SEM, n= 4. Means are significantly differ; P<0.05**

Table 2 represents the concentration of YC/rGO sample required to inhibit ABTS scavenging activity

by 50% and was determined to be  $155.28 \pm 2.16$  µg/ml. Therefore, YC/rGO shows higher antioxidant



activity. It confirmed that even a very small amount of YC/rGO composite is enough for considerable inhibition of ABTS radical scavenging activity.

Most molecules that have the potential to inhibit the radical scavenging activity of ABTS and DPPH are found to be hydrogen donors. Those antioxidants (AH) react with radicals (R<sup>•</sup>), ABTS<sup>•</sup> and DPPH<sup>•</sup>, like below.<sup>31</sup>



And form new radical A<sup>•</sup>, which no longer propagates radical chain reaction since it is sufficiently stable. It is interesting that the GO used in this study has shown low antioxidant activity compared to the YC/rGO and MC/rGO nanocomposites. Since GO is a

poor hydrogen donor, even though it consists of a higher amount of hydroxyl content when compared with the YC/rGO and MC/rGO nanocomposites.

It is believed that GO is considered as a poor hydrogen donor antioxidant due to its structure. Phenolic compounds, which are considered as potential antioxidants, form resonance structures for stable radicals after the donation of hydrogen. When considering the accepted structure of GO, basal sites are where OH groups are placed. In those regions, local sp<sup>3</sup> sites are created by C=C bond oxidation. Therefore, those sites do not facilitate the stabilization of radical resonances. As a result of those basal hydroxyl groups, satisfactory antioxidant activity from GO cannot be expected.<sup>31</sup>

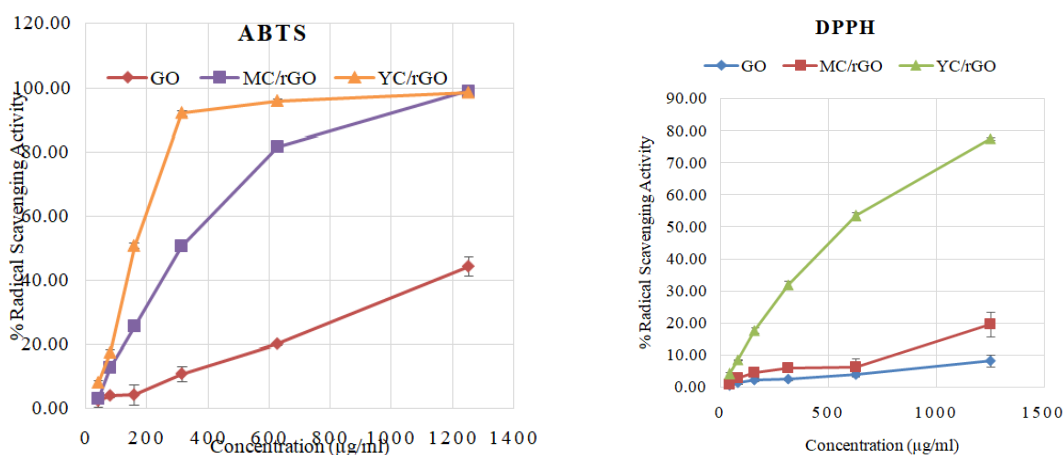


**Fig.10: Dose response relationship of YC/rGO and MC/rGO and GO (a) for ABTS assay and (b) GO for DPPH assay**

Figure 10 (a) and (b), illustrate that the ABTS and DPPH radical scavenging activities of YC/rGO and MC/rGO and GO are dose dependent. With increasing sample concentration, the percentage of radical scavenging increases.

Data represented as mean  $\pm$  SEM, n = 4. Means are significantly differ; P < 0.05.

In the course of inflammation, lysosomal enzymes are released at the sites, which results in damage to the tissues and organelles that surround them. There are so many methods used to screen the anti-inflammatory potential of various drugs, plant extracts and chemicals. These methods

include inhibiting protein denaturation, stabilization of lysosomal membrane, platelet aggregation, fibrinolytic assay and stabilization of the erythrocyte membrane.<sup>32,33</sup>

In this study, stabilization of heat-induced haemolysis of erythrocytes is used as a biochemical index to screen for anti-inflammatory activity.<sup>17</sup> Rabbit blood was taken for this assay. Since it is very similar to human blood.<sup>34</sup>

At different concentrations, all the test samples were inhibited by heat induced hemolysis, except for the chemically reduced GO. It may be due to its poor solubility in saline. These findings confirm

that the stabilization of the erythrocyte membrane is an additional mechanism in the anti-inflammation process. At the site of inflammation, these extracts may probably inhibit the release of lysosomal

enzymes. These lysosomal enzymes contain protease and bactericidal enzymes, which lead to further tissue damage and inflammation upon extracellular release.<sup>35</sup>

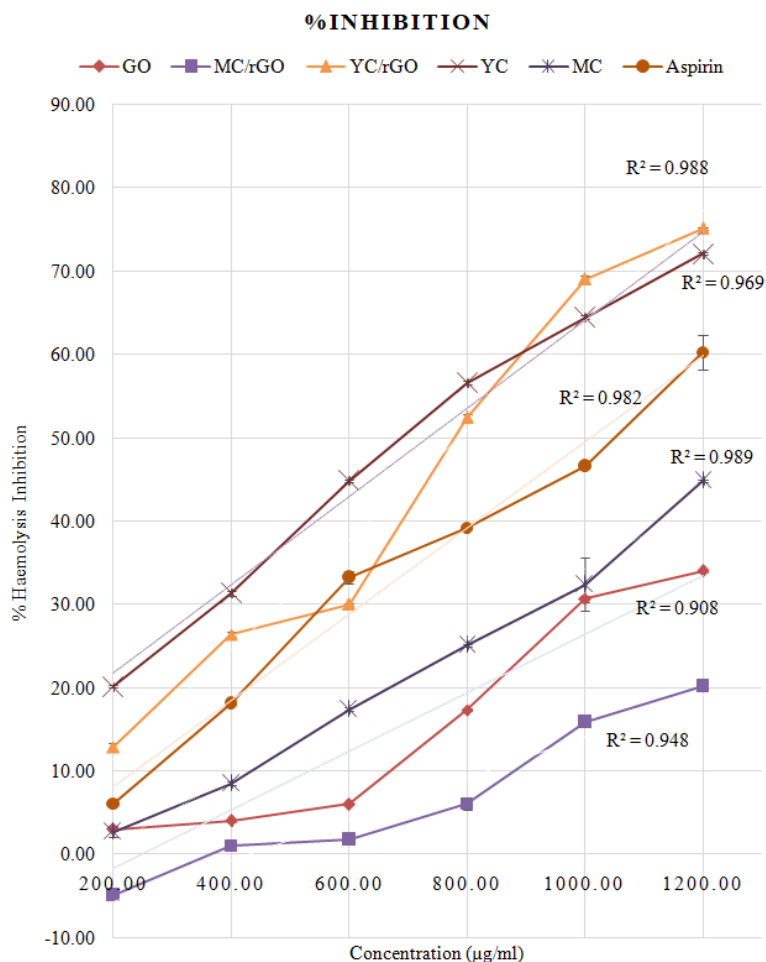


**Fig.11: Dose response relationship of heat induced membrane stabilization activity**  
 Data represented as mean ±SEM, n= 3. Means are significantly differ; P<0.05.

In a dose dependent manner, test extracts were able to protect red blood cells against heat induced lysis (Figure 11) and the inhibition potential was comparable with the NSAID, Aspirin. YC/rGO reported a maximum inhibition of 75.15± 0.14% at 1200µg/ml. The IC<sub>50</sub> of YC/rGO was obtained at 784.09±2.68 µg/ml at a correlation coefficient value (r<sup>2</sup>) of 0.97 (Table 3). The standard drug, aspirin was reported with a maximum inhibition of 60.24± 2.11% at 1200 µg/ml. Because MC/rGO has a -4.85 ± 0.32% at 200 µg/ml, it induces erythrocyte lysis at low concentrations. Moreover, MC/rGO showed the

minimum inhibition potential against heat induced lysis of erythrocytes, since MC/rGO obtained the highest IC<sub>50</sub> at 2437.50±17.52 µg/ml (r<sup>2</sup> = 0.98).

As shown in Figure 11, when considering YC and MC extracts, YC showed an overall higher inhibition potential than the MC extract. It is same as antioxidant activity of *C. arabica* leaves, the anti-inflammatory activity might also due to the phenols contain in coffee leaves. Age of the leaves have high impact on phenolic contents. And it was explained that the phenolic content in younger leaves is higher

than in mature leaves. Hence young *C.arabica* leaves have greater anti-inflammatory potential than mature leaves.<sup>3</sup> This scenario also can be found in YC/rGO and MC/rGO.

**Table 3: Heat induced membrane stability activity**

% Inhibition	
Test Sample	Membrane stabilization (IC <sub>50</sub> )/ µg/ml
YC	730.91± 1.86
YC/rGO	784.09±2.68
Aspirin (why?)	1020.96±7.43
MC	1423.60±14.84
GO	1673.06±12.67
MC/rGO	2437.50±17.52

Values are represented as mean ± SEM, n= 3/ concentration. YC: young *C.arabica* leaf extract, YC/rGO: young *C.arabica*/reduced graphene oxide composite, MC/rGO: matured *C.arabica* /reduced graphene oxide composite, GO: graphene oxide. MC: mature *C.arabica* leaf extract.

The correlation coefficient for YC and YC/rGO was found to be 0.98. Therefore the dose dependent inhibition against hemolysis of erythrocytes of YC and YC/rGO, was closely related. During the anti-inflammatory action of reduced GO, membrane stabilization mainly occurs by inhibiting the metabolism of arachidonic acid. It resulted in preventing the action of lipoxygenase, phospholipase A2 and cyclooxygenase. Therefore, a shielding effect was provided towards the inflammatory response.<sup>37</sup> Based on the findings, YC/rGO was found to be an effective candidate for anti-inflammatory action. The GO also showed a maximum inhibition of 34.00±0.18% at 1200 µg/ml. It is higher than the anti-inflammatory potential of MC/rGO.

A feasible explanation for the erythrocyte membrane stabilization of YC/rGO could be due to interactions with membrane proteins, shrinkage of the cell or expansion of the membrane, which leads to increase in the surface area/volume ratio of the cells. And it has been shown the intercellular calcium contents

are closely related with cell volume and deformability of erythrocytes. Therefore, it may be hypothesized that the ability of the leaf extracts and *C.arabica*/rGO nanocomposites to alter the influx of calcium into the cells will lead to stabilize the erythrocyte membrane.<sup>37</sup> The present study proposes that the membrane stabilizing activity of YC/rGO may play a remarkable role in its anti-inflammatory activity.

### Conclusion

Employing a cost-effective and eco-friendly method, graphite oxide (GO) was successfully reduced to reduced graphene oxide (rGO) for the first time by using *Coffea arabica* leaf extract as a green reducing agent, and the formation was verified through Raman, XRD and SEM. The antioxidant and anti-inflammatory activities of the coffee young, as well as matured leaves - rGO composites, were investigated. *Coffea arabica* young leaves /rGO nanocomposite shows good antioxidant properties and anti-inflammatory properties compared with that of matured leaf rGO nanocomposite. Such significant antioxidant and anti-inflammatory properties of a plant-based rGO nanocomposite have not been reported previously to the best of our knowledge. Although rGO / coffee seeds nanocomposites have been studied coffee leaves /rGO nanocomposite or its said properties have not been studied either.

The present study reveals that the young *Coffea arabica*/rGO nanocomposite can be used to design an effective antioxidant and anti-inflammatory drug which can be applied to healing various inflammation and aging diseases. It is expected to further optimize the antioxidant and anti-inflammatory properties of young *Coffea arabica*/rGO nanocomposite for biomedical applications in the future.

### Acknowledge

I would like to express my gratitude to Faculty of Graduate studies, University of Sri Jayewardenepura for granting permission to do my M.Sc. research. The Material technology and herbal sections of Industrial technology Institute are much praised for permitting laboratory work. I am also appreciative to the Department of Biochemistry, Faculty of Medical Sciences, University of Sri Jayewardenepura, Sri Lanka.

**Funding**

Financial support was provided by NRC Grant No 12-022 and No.16/138.

**Conflict of interest**

There is no conflict of interests regarding the publication of this article.

**References**

- de Almeida RF, Trevisan MTS, Thomaziello RA, Breuer A, Klika KD, Ulrich CM, et al. Nutraceutical compounds: Echinoids, flavonoids, xanthenes and caffeine identified and quantitated in the leaves of *Coffea arabica* trees from three regions of Brazil. *Food Res Int*. 2019;115(September 2018):493–503.
- Chen X. A review on coffee leaves: Phytochemicals, bioactivities and applications. *Crit Rev Food Sci Nutr* [Internet]. 2019;59(6):1008–25. Available from: <https://doi.org/10.1080/10408398.2018.1546667>
- Chen XM, Ma Z, Kitts DD. Effects of processing method and age of leaves on phytochemical profiles and bioactivity of coffee leaves. *Food Chem* [Internet]. 2018;249(September 2017):143–53. Available from: <https://doi.org/10.1016/j.foodchem.2017.12.073>
- Raimond JM, Brune M, Computation Q, Martini F De, Monroe C. Electric Field Effect in Atomically Thin Carbon Films. *2004*;306(October):666–70.
- Liu C, He C, Xie T, Yang J. Reduction of graphite oxide using ammonia solution and detection of Cr(VI) with graphene-modified electrode. *Fullerenes Nanotub Carbon Nanostructures*. 2015;23(2):125–30.
- Suresh D, Udayabhanu, Pavan Kumar MA, Nagabhushana H, Sharma SC. Cinnamon supported facile green reduction of graphene oxide, its dye elimination and antioxidant activities. *Mater Lett* [Internet]. 2015;151:93–5. Available from: <http://dx.doi.org/10.1016/j.matlet.2015.03.035>
- Chen X, Mu K, Kitts DD. Characterization of phytochemical mixtures with inflammatory modulation potential from coffee leaves processed by green and black tea processing methods. *Food Chem* [Internet]. 2019;271(March 2018):248–58. Available from: <https://doi.org/10.1016/j.foodchem.2018.07.097>
- Hummers WS, Offeman RE. Preparation of Graphitic Oxide. *J Am Chem Soc*. 1958;80(6):1339.
- Marcano DC, Kosynkin DV, Berlin JM, Sinitskii A, Sun Z, Slesarev AS, et al. Correction to Improved Synthesis of Graphene Oxide. *ACS Nano*. 2018;12(2):2078–2078.
- Muzyka R, Kwoka M, Smęadowski Ł, Díez N, Gryglewicz G. Oxidation of graphite by different modified Hummers methods. *Xinxing Tan Cailiao/New Carbon Mater*. 2017;32(1):15–20.
- Yoo MJ, Park HB. Effect of hydrogen peroxide on properties of graphene oxide in Hummers method. *Carbon N Y* [Internet]. 2019;141:515–22. Available from: <https://doi.org/10.1016/j.carbon.2018.10.009>
- Pham VH, Hur SH, Kim EJ, Kim BS, Chung JS. Highly efficient reduction of graphene oxide using ammonia borane. *Chem Commun*. 2013;49(59):6665–7.
- Blois MS. Antioxidant determinations by the use of a stable free radical [10]. *Nature*. 1958;181(4617):1199–200.
- Activity A, An A, Abts I, Assay CD. ANTIOXIDANT ACTIVITY APPLYING AN IMPROVED ABTS RADICAL. 1999;26(98):1231–7.
- Leelaprakash G, Mohan Dass S. In vitro anti-inflammatory activity of methanol extract of *enicostemma axillare*. *Int J Drug Dev Res*. 2011;3(3):189–96.
- Perez RM, Perez S, Zavala MA, Salazar M. Anti-inflammatory activity of the bark of *Hippocratea excelsa*. *J Ethnopharmacol*. 1995;47(2):85–90.
- Zhou M, Guo L ping, Lin F yun, Liu H xia. Electrochemistry and electrocatalysis of polyoxometalate-ordered mesoporous carbon modified electrode. *Anal Chim Acta*. 2007;587(1):124–31.
- Suresh D, Nethravathi PC, Udayabhanu A, Nagabhushana H, Sharma SC. Spinach assisted green reduction of graphene oxide and its antioxidant and dye absorption properties. *Ceram Int* [Internet].

- 2015;41(3):4810–3. Available from: <http://dx.doi.org/10.1016/j.ceramint.2014.12.036>
19. Thakur S, Karak N. Green reduction of graphene oxide by aqueous phytoextracts. *Carbon N Y*. 2012;50(14):5331–9.
  20. Moosa A, Noori Jaafar J. Green Reduction of Graphene Oxide Using Tea Leaves Extract with Applications to Lead Ions Removal from Water. *Nanosci Nanotechnol*. 2017;7(2):38–47.
  21. Thakur S, Karak N. Green reduction of graphene oxide by aqueous phytoextracts. *Carbon N Y* [Internet]. 2012;50(14):5331–9. Available from: <http://dx.doi.org/10.1016/j.carbon.2012.07.023>
  22. Jana M, Saha S, Khanra P, Murmu NC, Srivastava SK, Kuila T, et al. Bio-reduction of graphene oxide using drained water from soaked mung beans (*Phaseolus aureus* L.) and its application as energy storage electrode material. *Mater Sci Eng B Solid-State Mater Adv Technol* [Internet]. 2014;186(1):33–40. Available from: <http://dx.doi.org/10.1016/j.mseb.2014.03.004>
  23. Taylor P, Billes F, Ziegler IM. Vibrational Spectroscopy of Phenols and Phenolic Polymers . Theory , Experiment , and Applications. 37–41 p.
  24. Wang J, Salihi EC, Šiller L. Green reduction of graphene oxide using alanine. *Mater Sci Eng C*. 2017;72:1–6.
  25. Stankovich S, Dikin DA, Piner RD, Kohlhaas KA, Kleinhammes A, Jia Y, et al. Synthesis of graphene-based nanosheets via chemical reduction of exfoliated graphite oxide. *Carbon N Y*. 2007;45(7):1558–65.
  26. Fu C, Zhao G, Zhang H, Li S. Evaluation and Characterization of Reduced Graphene Oxide Nanosheets as Anode Materials for Lithium-Ion Batteries. 2013;8:6269–80.
  27. Enadis NIN, Ang LANENW, Simidou MAT, Hang HONGUZ. Estimation of Scavenging Activity of Phenolic Compounds Using the ABTS • + Assay. 2004;4669–74.
  28. Patay ÉB, Bencsik T, Papp N. Phytochemical overview and medicinal importance of *Coffea* species from the past until now. *Asian Pac J Trop Med* [Internet]. 2016 Dec 1 [cited 2020 Mar 8];9(12):1127–35. Available from: <https://www.ncbi.nlm.nih.gov/pubmed/27955739>
  29. Vuolo MM, Lima VS, Roberto M, Junior M. Classification , and Antioxidant Power [Internet]. *Bioactive Compounds*. Elsevier Inc.; 2019. 33–50 p. Available from: <https://doi.org/10.1016/B978-0-12-814774-0.00002-5>
  30. Salgado PR, Favarin JL, Leandro RA, De Lima Filho OF. Total phenol concentrations in coffee tree leaves during fruit development. *Sci Agric*. 2008;65(4):354–9.
  31. Qiu Y, Wang Z, Owens ACE, Kulaots I, Chen Y, Kane AB, et al. Antioxidant chemistry of graphene-based materials and its role in oxidation protection technology. *Nanoscale*. 2014;6(20):11744–55.
  32. Oyedapo O. Red blood cell membrane stabilizing potentials of extracts of *Lantana camara* and its fractions. *Int J Plant Physiol Biochem* [Internet]. 2010;2(October):46–51. Available from: [http://www.academicjournals.org/ijppb/PDF/PDF\\_2010/Oct/Oyedapo\\_et\\_al.pdf](http://www.academicjournals.org/ijppb/PDF/PDF_2010/Oct/Oyedapo_et_al.pdf)
  33. PAL S, SEN T, CHAUDHURI AKN. Neuropsychopharmacological Profile of the Methanolic Fraction of *Bryophyllum pinnatum* Leaf Extract . *J Pharm Pharmacol*. 1999;51(3):313–8.
  34. Shiomi M. Rabbit as a model for the study of human diseases. *Rabbit Biotechnol Rabbit Genomics, Transgenesis, Cloning Model*. 2009;49–63.
  35. Chou CT. The antiinflammatory effect of an extract of *Tripterygium wilfordii* Hook F on adjuvant-induced paw oedema in rats and inflammatory mediators release. *Phyther Res*. 1997;11(2):152–4.
  36. Liu K, Wang Y, Li H, Duan Y. A facile one-pot synthesis of starch functionalized graphene as nano-carrier for pH sensitive and starch-mediated drug delivery. *Colloids Surfaces B Biointerfaces* [Internet]. 2015;128:86–93. Available from: <http://dx.doi.org/10.1016/j.colsurfb.2015.02.010>
  37. Shinde UA, Phadke AS, Nair AM, Mungantiwar AA, Dikshit VJ, Saraf MN. Membrane stabilizing activity - A possible mechanism of action for the anti-inflammatory activity of *Cedrus deodara* wood oil. *Fitoterapia*. 1999;70(3):251–7.